Supplementary materials for

Escape from breast tumor dormancy: The convergence of obesity and menopause

Roopali Roy[1,2,*], Jiang Yang[1,2], Takaya Shimura[1,2], Lauren Merritt[1], Justine Alluin[1], Emily Man[1], Cassandra Daisy[1], Rama Aldakhlallah[1], Deborah Dillon[3], Susan Pories[4,5], Lewis A. Chodosh[6] and Marsha A. Moses[1,2,*]

Corresponding author: Email: marsha.moses@childrens.harvard.edu; Roopali.roy@childrens.harvard.edu

This file includes

Supplementary Materials and Methods

Supplementary figures

Supplementary tables

Animals and animal care

All animal studies were performed according to the protocols approved by the Institutional Animal Care and Use Committees of Boston Children's Hospital. Mice were housed in Association for Assessment and Accreditation of Laboratory Animal Care International (AALAC)–accredited facilities. SCID mice for the orthotopic tumor studies were purchased from MGH and Jackson Laboratory. FvB mice were purchased from Charles River Laboratory and then bred (to create transgenic mice as described below) and maintained in the animal facility. For all animal studies, mice were randomly selected and quantitative and imaging measurements were conducted on all mice without any introduction of bias.

Breast tumor models

7 wk old female mice were ovariectomized (ovx) as described previously (*1*) to establish PM status. Mice in both tumor models were then randomized and placed either on NC (normal chow; D12450B, 10% kcal fat, Research Diets, Inc.) or DIO (diet-induced obesity; D12492, 60% kcal fat, Research Diets, Inc., New Brunswick, NJ) diet for 5-7 weeks. All mice were given food and water *ad libitum*. Body weights were monitored and when DIO mice had attained ≥1.5-fold higher mean weight compared to NC mice tumor studies were commenced. Mouse BMI was calculated as weight/length (head to hind legs). Diet regimens (DIO or NC) were continued throughout the duration of study.

Orthotopic breast tumor xenografts: Luciferase-labeled MDA-MB-436P cells (2×10^6) were orthotopically injected into the fourth right inguinal MFP (*2, 3*) of female PM SCID mice maintained on DIO or NC regimens. Mice were monitored and tumors measured with calipers (palpation) or by IVIS (BLI) imaging weekly. Mice were anesthetized (2-4% isoflurane by inhalation) and injected with luciferin prior to imaging. Mice were euthanized when tumors reached 1 cm or when mice were moribund for the end point (EP) study and after 5 wks in the early time point (ETP) study.

Transgenic model: We have utilized an inducible Wnt bitransgenic mouse model that develops spontaneous mammary tumors. The MMTV-rtTA-pA (MTB) and TetO-Wnt-IRES-Luciferase (TWNT) mouse lines were obtained from Dr. Lewis Chodosh and crossed to create the bitransgenic MTB-TWNT model that expresses the mammary specific reverse tetracycline transactivator (rtTA) and the Wnt/luciferase transgenes under the control of a tetracycline operator (*4, 5*). Following doxycycline treatment, >90% of these mice (MTB/TWNT) develop mammary adenocarcinomas with median latency of ~20 weeks (*5*). *WNT* transgene activation was induced via 2 mg/ml doxycycline administration in the drinking water and continued throughout the study. Tumor growth was monitored via IVIS imaging weekly or with calipers when they became palpable (EP study). For the ETP study, mammary fat pad (MFP) displaying a BLI signal (n ≥3/group/time point) were collected between wks 3 – 9 and analyzed. Sunitinib treatment studies were conducted on the MTB-TWNT DIO mice. Sunitinib (LC Laboratories, Woburn MA) (dissolved in 4% DMSO, 30% PEG300) (n=8) or Vehicle (n=10) was administered by oral gavage at a dose of 80 mg/kg 3 days a week starting 1 week after *WNT* transgene activation as described previously (*6, 7*). Body weight and BLI were monitored. At 10 wks MFPs and associated tumors were harvested and analyzed.

Cell lines and reagents

We have utilized human BC cell lines derived from dormant and active breast tumors. The dormant (MDA-MB-436P) and highly angiogenic (MDA-MB-436A) cell lines were the kind gift of Dr. Judah Folkman (*8-10*). When tested *in vivo*, MDA-MB-436P cells have a prolonged dormancy period whereas the MDAMB436A cells have a much shorter one (*9*). MCF-7, MDA-MB-231 and T47D breast cancer cells (American Type Culture Collection, ATCC, Manassas, VA) were cultured according to ATCC protocols in Dulbecco's modified Eagle's medium (DMEM) with 10% fetal bovine serum (FBS) as per protocol. Human dermal microvascular endothelial cells (HMVEC; Lonza, Walkersville, MD) were cultured in EGM-2™ MV Microvascular Endothelial SingleQuots™ Kit (Lonza) as per Lonza's protocol. Preadipocytes (subcutaneous) obtained from an obese, PM female donor (BMI ≥ 30; Age; 57 yr.; Cell Applications Inc., San Diego, CA) were cultured in HPAd Growth Medium (Cell Applications Inc.), differentiated into mature adipocytes and maintained as per

Cell Application's protocol. Adipocyte conditioned medium (ObAdCM) was prepared using HPAd starvation medium (Cell Applications Inc.) with each batch of adipocytes conditioned three times with 24-48 h incubation in maintenance medium between collections. Unconditioned medium (UCM) was used as the control. Cells in culture were routinely tested for mycoplasma and if positive were discarded or treated until mycoplasma-free.

Functional assays

Cell proliferation: 1 x 10^4 BC cells were seeded per well in DMEM with 10% FBS in 96-well plates. Cell viability was analyzed 72 hours later using Cell Counting Kit-8 (Dojindo Molecular Technologies, Rockville, MD) as previously described (*3, 11*).

Cell migration and invasion: Migration and invasion assays were conducted as described previously (*2, 3*). Briefly, 5 x 10^4 BC cells were seeded per well in DMEM in the upper chamber (Costar Transwell®, Corning Inc., Corning, NY). ObAdCM, unconditioned medium (UCM) or full medium (FM; containing 10% FBS) was placed in the lower chamber. After 24 h, cells were fixed in 10% formalin and stained with 0.05% crystal violet. Adherent cells on the bottom of the filter were counted. For invasion BC cells were seeded in BioCoat™ Matrigel® Invasion Chambers (BD Biosciences) and assay conducted as described previously (*2*).

Endothelial cell recruitment assay: 6 x 10^4 BC cells were seeded into 24-well plates and treated with ObAdCM or UCM for 24 h. Subsequently, BC cells were washed with PBS and maintained in serum-free EBM-2 containing 0.1% BSA overnight. 5 x 10^4 human microvascular endothelial cells (HMVEC) were plated in the upper transwell chamber in serum-free EGM-2. After 18 h, migrated HMVEC were stained and counted as described previously (*11*).

Immunoblot analysis and antibodies

Cell lysates were prepared using 1X lysis buffer (Cell Signaling Technology). Protein concentration of lysates and CM were determined using the Bradford method (Biorad Laboratories, Hercules, CA) as previously described (*2, 12, 13*). Immunoblotting was conducted as described previously (*2, 11, 13*). Antibodies used included: phospho-STAT3/total STAT3, phospho-MAPK/total MAPK, and phospho-Akt/total Akt (Cell

Signaling Technology, Danvers, MA), β-actin (Abcam, Cambridge, MA); ERα (Santa Cruz Biotechnology, Santa Cruz, CA) and HRP-conjugated anti-rabbit and anti-mouse antibodies (Vector Biolabs, Burlingame, CA).

Histology and immunostaining

Tumor sections were blinded then classified on the basis of cellular morphology and arrangement by a pathologist. Hyperplastic ducts contained three or more layers of MECs, and 10 ducts/gland were analyzed. Adipocyte diameters were measured from 10 adipocytes/image on 5 images/MFP. Crown-like structures were quantified using tissue sections stained with anti-F4/80. IHC was performed on formalin-fixed tumors (3-5/group) for EP and ETP studies respectively. Endogenous peroxidase activity was inhibited with 3% hydrogen peroxide for 10 min. Antigen retrieval was performed with 10mM citrate buffer for 15 min in a microwave oven and then followed by a 2 min cool down at RT. H & E, VEGF (ab52917; R&D systems), LCN2 (AF1757; LSBio, Seattle, WA) and Tsp-1 (ab85762; 85762, Abcam) staining was performed as described previously (*3*). Whole tumor sections were imaged (4x resolution) on an Echo rebel microscope (ECHO, Sandiego CA). Higher magnification brightfield and fluorescent images were imaged using a Zeiss Axios microscope (Zeiss, Whiteplains NY).

Adipokine and cytokine analysis

For mouse serum, blood was collected via cardiac puncture at EP of study and incubated at RT for 15 min in BD Microtainer capillary blood collector (Fisher Scientific) followed by centrifugation at 1300 RPM for 5 min. Serum was stored at -80°C. Total protein was determined using the Bradford method (Biorad Laboratories, Hercules, CA) as previously described (*2, 12, 13*). Monospecific ELISAs for VEGF, LCN2, IL-6, bFGF, Tsp-1 (R&D Systems, Inc., Minneapolis, MN, USA), 17β-estradiol (Abcam, Cambridge, MA) were performed according to manufacturer's instructions. All analyses were conducted in duplicate and values with coefficients of variation (CV) >25% were excluded according to manufacturer recommendations.

Supplementary Figures

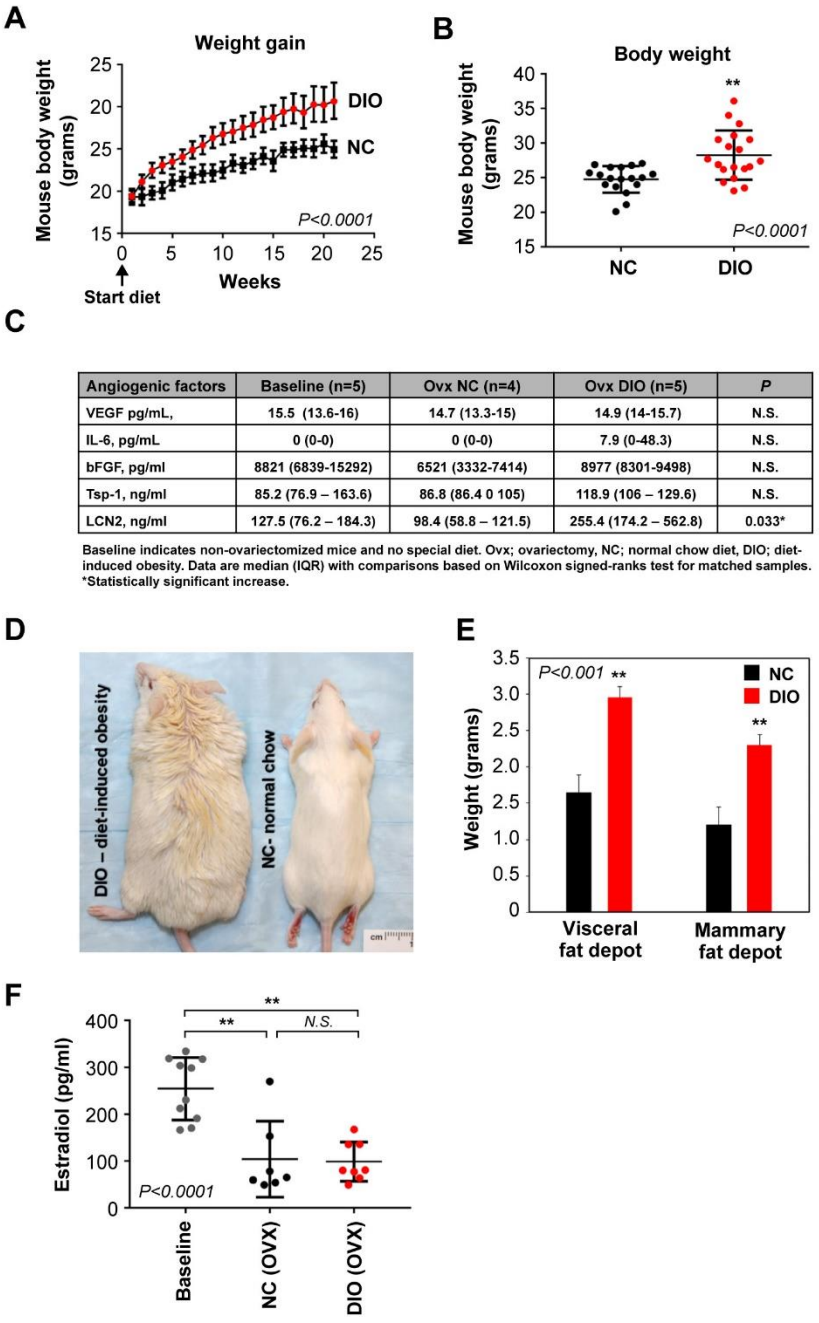

Angiogenic factors	Baseline (n=5)	Ovx NC (n=4)	Ovx DIO (n=5)	*P*
VEGF pg/mL,	15.5 (13.6-16)	14.7 (13.3-15)	14.9 (14-15.7)	N.S.
IL-6, pg/mL	0 (0-0)	0 (0-0)	7.9 (0-48.3)	N.S.
bFGF, pg/ml	8821 (6839-15292)	6521 (3332-7414)	8977 (8301-9498)	N.S.
Tsp-1, ng/ml	85.2 (76.9 – 163.6)	86.8 (86.4 0 105)	118.9 (106 – 129.6)	N.S.
LCN2, ng/ml	127.5 (76.2 – 184.3)	98.4 (58.8 – 121.5)	255.4 (174.2 – 562.8)	0.033*

Baseline indicates non-ovariectomized mice and no special diet. Ovx; ovariectomy, NC; normal chow diet, DIO; diet-induced obesity. Data are median (IQR) with comparisons based on Wilcoxon signed-ranks test for matched samples. *Statistically significant increase.

Figure S1. DIO promotes obesity and systemic angiogenic changes. Mice (SCID) fed with the DIO versus NC diet maintained significantly higher body weight throughout the study (**A**; n=21/group, Mann Whitney test, *P*<0.0001) and at end point (**B**; wk 23; n=19/group, Student's t test, *P*<0.0001). Serum levels of angiogenic factors in baseline non-ovariectomized (ovx) controls, and ovx NC and DIO FvB mice (**C**). Representative DIO and NC mice (**D**). Visceral and MFP depots in DIO mice weighed more than in NC mice (**E**; wk 13, Student's t test, *P*<0.001). Estradiol levels were significantly lower in ovx NC and DIO mice as compared to non-ovx

controls (**F**; one way ANOVA, *P*<0.0001), whereas levels did not differ significantly between ovx NC and DIO groups. All error bars indicate mean ± SEM.

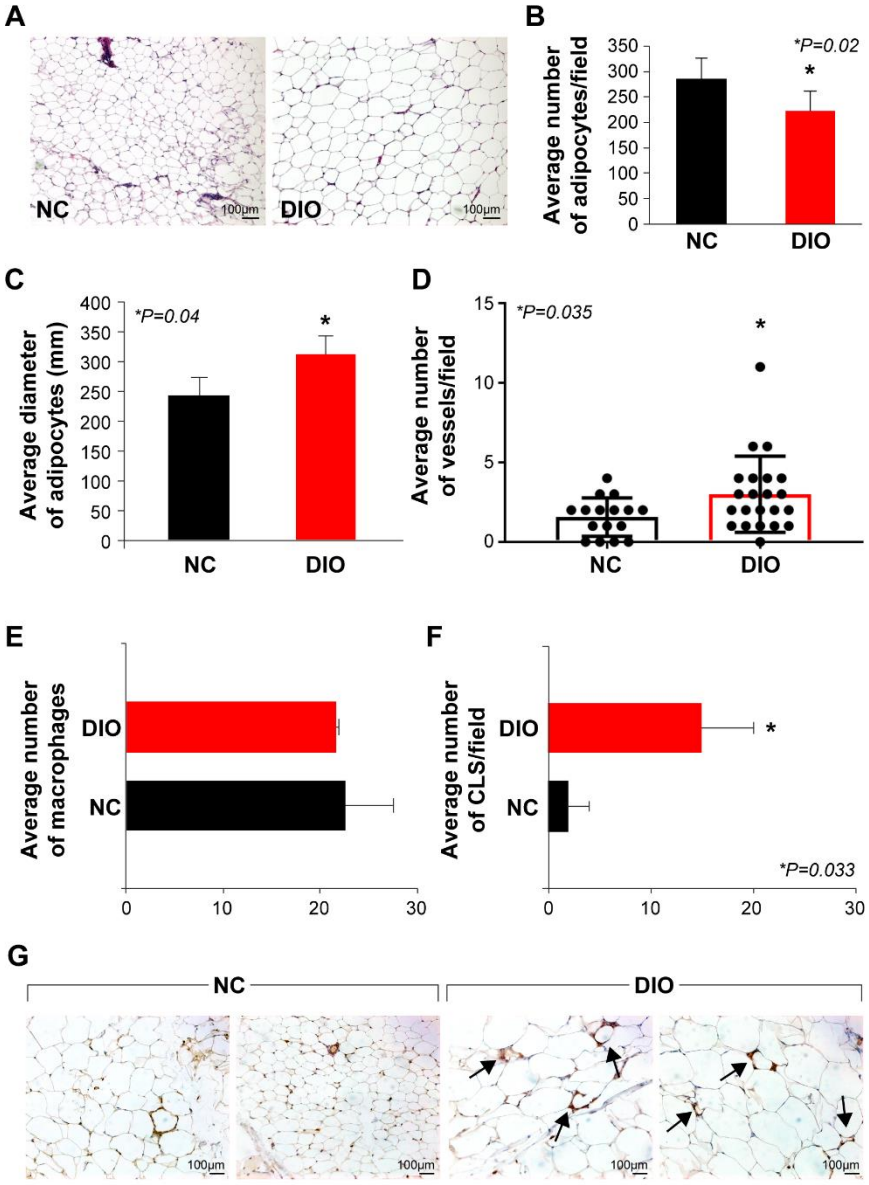

Figure S2. **MFP of DIO mice at baseline displayed hypertrophic adipocytes and enhanced angiogenesis**. Representative MFP H&E section from DIO and NC groups (**A**). Average number of adipocytes (per field) were lower in DIO MFPs (**B**, n=5/group; Student's t test, *P*=0.02). Average diameter of adipocytes was significantly higher in the DIO MFPs (**C**, n=5/group; Student's t test, *P*=0.04). Microvessel density (CD31+) was higher in DIO MFP (**D**, n=4/group, Student's t test, *P*=0.035). Number of macrophages in the MFPs did not

differ significantly between NC and DIO groups (**E**). DIO MFP had significantly higher numbers of crown-like structures (CLS) (**F-G**, Student's t test, *P*=0.033). Black arrows indicate CLS (**G**).

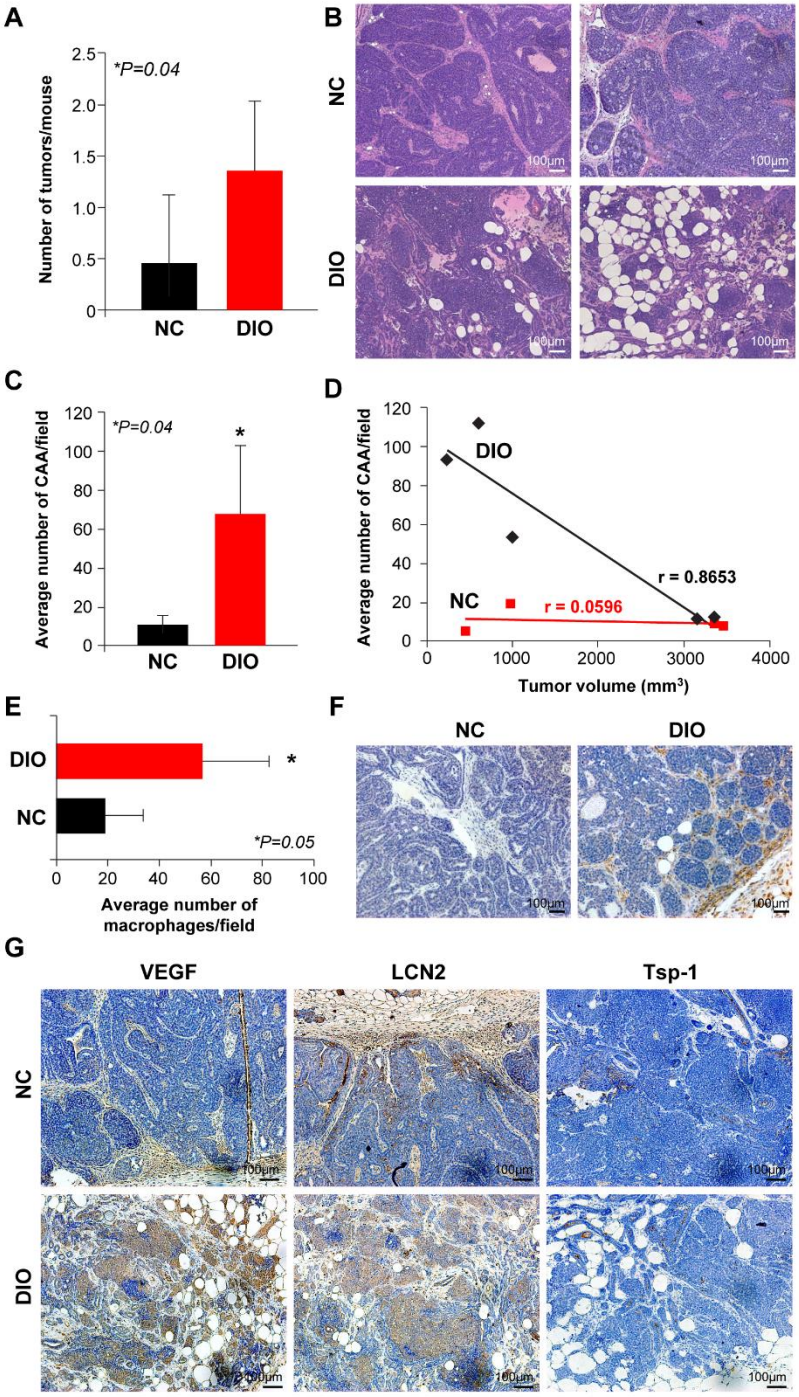

Figure S3. **DIO MTB-TWNT tumors have increased infiltration of cancer-associated adipocytes and macrophages**. DIO mice had a higher incidence of multiple tumors in different mammary glands compared to NC mice (**A**, EP study, n=10/group, Student's t test, *P*=0.04). Tumors in DIO mice displayed increased

infiltration of adipocytes (**B-C**, n=6/group, Student's t test, *P*=0.04). Representative H&E sections of tumors from NC and DIO groups (**B**). There was an inverse correlation between tumor size and adipocyte infiltration in DIO mice but not in NC mice (**D**, Pearson r=0.8653). DIO tumors had significantly higher F480+ macrophages compared to NC tumors (**E-F**, n=6/group, Student's t test, *P*=0.05). Representative NC and DIO EP tumors indicating macrophage infiltration (**F**). DIO tumors had increased VEGF and LCN2 expression whereas Tsp-1 levels were low in both groups (**G**, n=3/group).

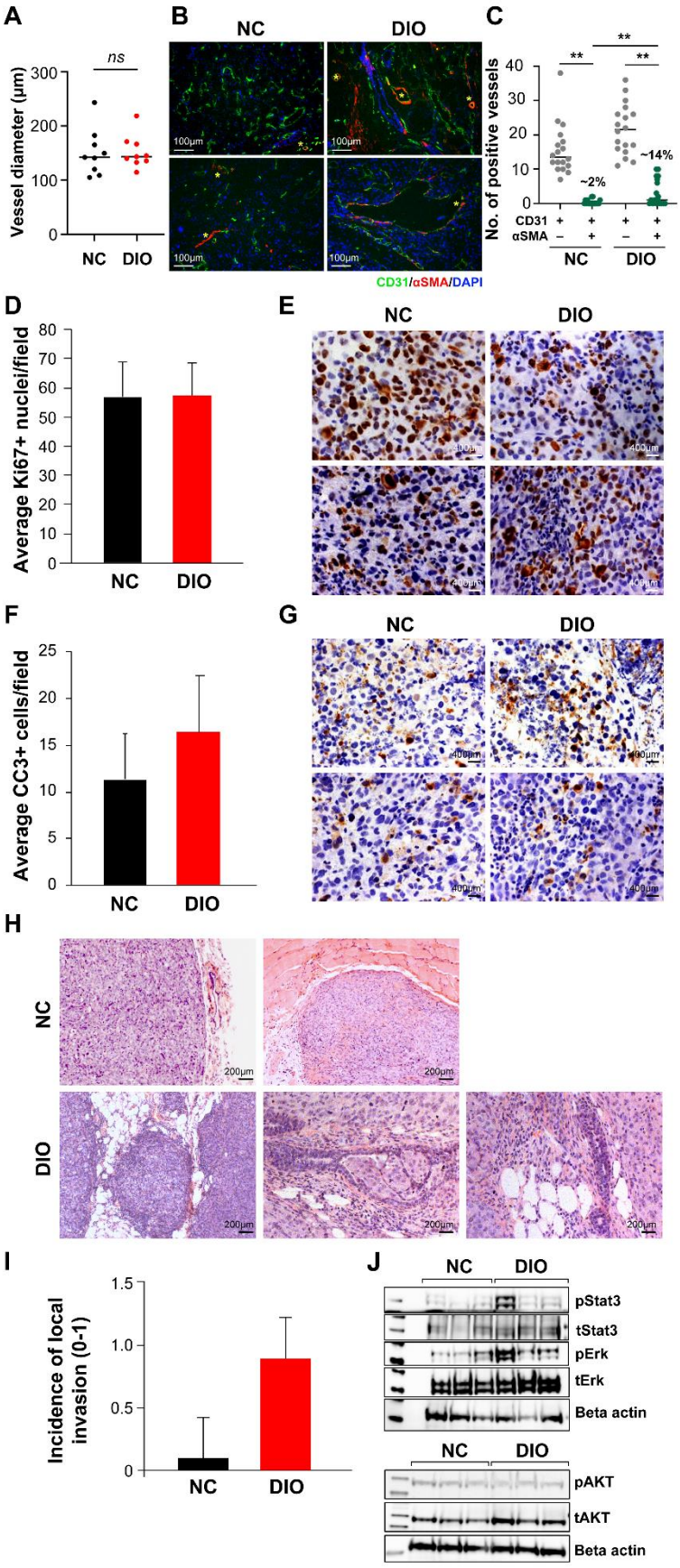
A
Vessel diameter (μm)
300
200
100
0
ns
NC
DIO
B
NC
DIO
100μm
CD31/αSMA/DAPI
C
No. of positive vessels
40
30
20
10
0
**
**
**
~2%
~14%
CD31 + + + +
αSMA – + – +
NC
DIO
D
Average Ki67+ nuclei/field
80
70
60
50
40
30
20
10
0
NC
DIO
E
NC
DIO
400μm
F
Average CC3+ cells/field
25
20
15
10
5
0
NC
DIO
G
NC
DIO
400μm
H
NC
DIO
200μm
I
Incidence of local invasion (0-1)
1.5
1.0
0.5
0
NC
DIO
J
NC
DIO
pStat3
tStat3
pErk
tErk
Beta actin
NC
DIO
pAKT
tAKT
Beta actin

Figure S4. **DIO MDA-MB-436P tumors demonstrated increased local invasion and activated STAT3 signaling**. Diameter of tumor blood vessels did not differ between the NC and DIO groups (**A**; each point represents average vessel diameter from six different fields, n=9/group). Pericyte coverage of tumor vessels was significantly higher in tumors from DIO mice (**B, C**). Representative IHC of tumor sections indicating CD31+ (endothelial cells) and αSMA+ (pericyte/mural cells) staining in tumor vessels (**B**). DIO tumors had a higher proportion of mature vessels with pericyte coverage (**C**; *denotes dual SMA/CD31 staining, DIO: 14% vs. NC: 2%, n=3-4 tumors/group, Student's t test, P=0.05). Tumor proliferation (Ki67+) did not differ between the NC and DIO groups (**D-G**, EP study). Representative tumor sections indicating Ki67+ nuclear staining (**E**, n=4/group). Apoptosis rates (cleaved caspase 3+ cells) did not differ between the NC and DIO groups (**F-G**, EP study). Representative tumor sections indicating CC3+ staining (**G**, n=4/group). Incidence of local invasion in the surrounding fat pad, muscle or blood vessels were higher in the DIO tumors (**H-I**, EP study, n=3/group, Student's t test, P=0.05). H&E sections indicated representative tumors, whereas NC tumors had distinct boundaries and no invasion into the surrounding stroma, DIO tumors tended to invade into the surrounding fat pad, local blood vessels and normal ducts (**H**). pSTAT3 and pErk levels were higher in DIO tumors whereas pAkt levels remained unchanged (**J**, n=3/group, beta actin was used as loading control).

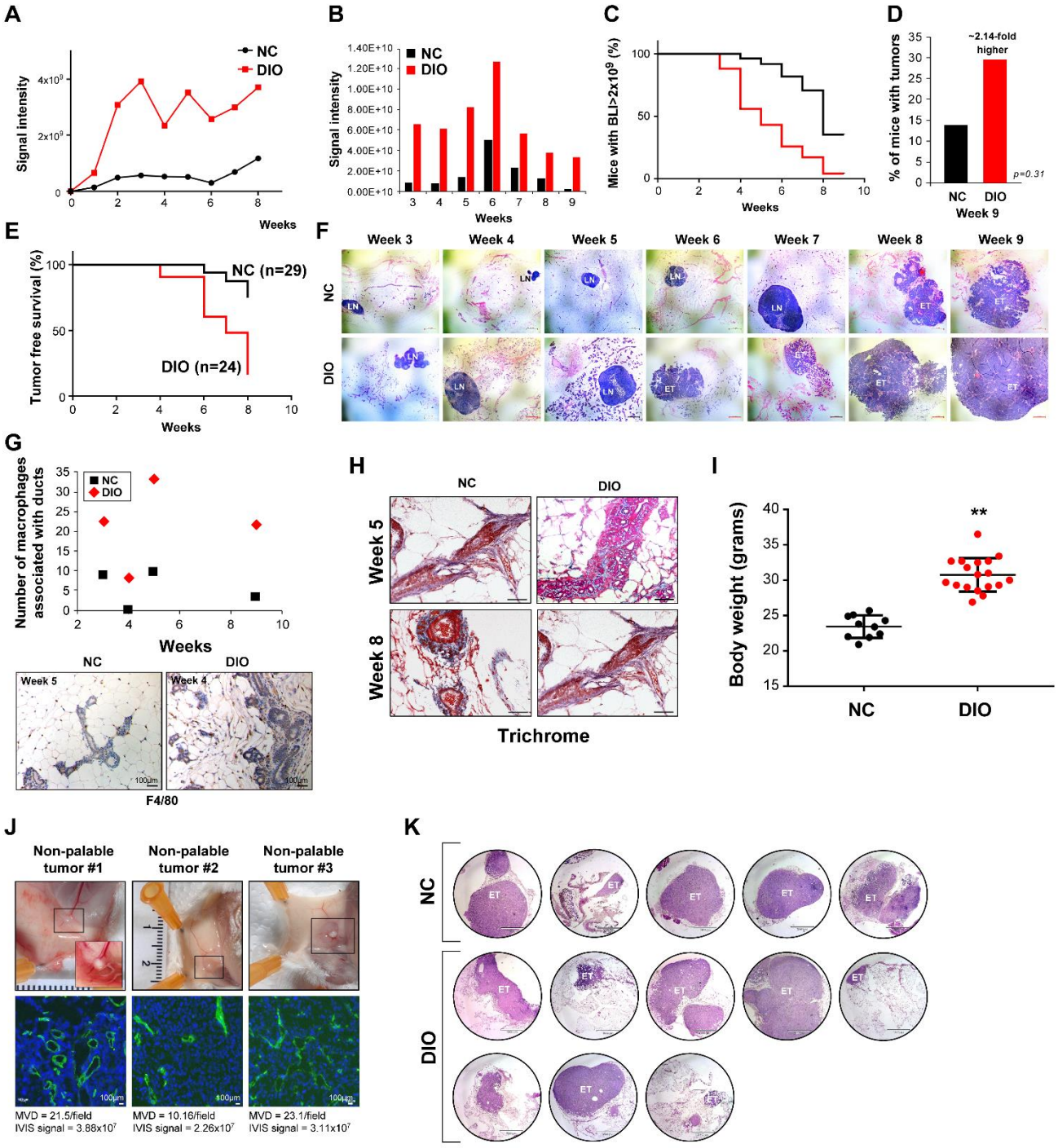
A
Signal intensity
NC
DIO
Weeks
B
Signal intensity
NC
DIO
Weeks
C
Mice with BLI>2x10^9 (%)
Weeks
D
% of mice with tumors
~2.14-fold higher
p=0.31
NC
DIO
Week 9
E
Tumor free survival (%)
NC (n=29)
DIO (n=24)
Weeks
F
Week 3
Week 4
Week 5
Week 6
Week 7
Week 8
Week 9
NC
DIO
LN
ET
G
Number of macrophages associated with ducts
NC
DIO
Weeks
NC
DIO
Week 5
Week 4
100μm
F4/80
H
NC
DIO
Week 5
Week 8
Trichrome
I
Body weight (grams)
**
NC
DIO
J
Non-palable tumor #1
Non-palable tumor #2
Non-palable tumor #3
100μm
MVD = 21.5/field
IVIS signal = 3.88x10^7
MVD = 10.16/field
IVIS signal = 2.26x10^7
MVD = 23.1/field
IVIS signal = 3.11x10^7
K
NC
DIO
ET

Figure S5. **DIO MTB-TWNT mice displayed accelerated tumor vascular switch-points and lower tumor-free survival at early time point (ETP) of tumor development**. Average BLI signal intensity was higher in DIO MFPs at all time point during the ETP study (**A-B**). Average BLI signal in each group at the indicated time (wk 3-9) (**B**, n=3-4/group). DIO MTB-TWNT MFP acquire the tumor vascular switch earlier than those in the NC group (**C**). Tumor frequency was two-fold higher in the DIO ETP study (**D**, N.S.). Tumor-free survival was significantly shorter in the DIO mice (**E**). H&E staining of representative MFPs from NC and DIO groups from the MTB-TWNT ETP study (week 3-9) indicating early tumor development (**F**; MFP 4x magnification, LN: lymph node, ET: early tumor). Hyperplastic ducts and neoplastic lesions in DIO MFP had increased macrophage infiltration compared to NC MFP in the ETP study (**G**). Representative sections of MFP indicating F480+ macrophage staining (**G**, lower panel). MFP in DIO mice had increased fibrous stroma around the hyperplastic and neoplastic ducts, trichrome staining of representative NC and DIO MFP indicated in the ETP study (**H**). Mice on the DIO regimen had higher body weight compared to the NC regimen in the MDA-MB-436P orthotopic (**I**, ETP study). Representative images of MDA-MD-436P non-palpable tumors harvested at week 5 (ETP study) and corresponding MVD analysis (CD31+) and associated BLI signal intensity (**J**). H&E staining of representative MFPs from NC and DIO groups from the MDA-MD-436P orthotopic ETP study (**K**; MFP 4x magnification, ET: early tumor).

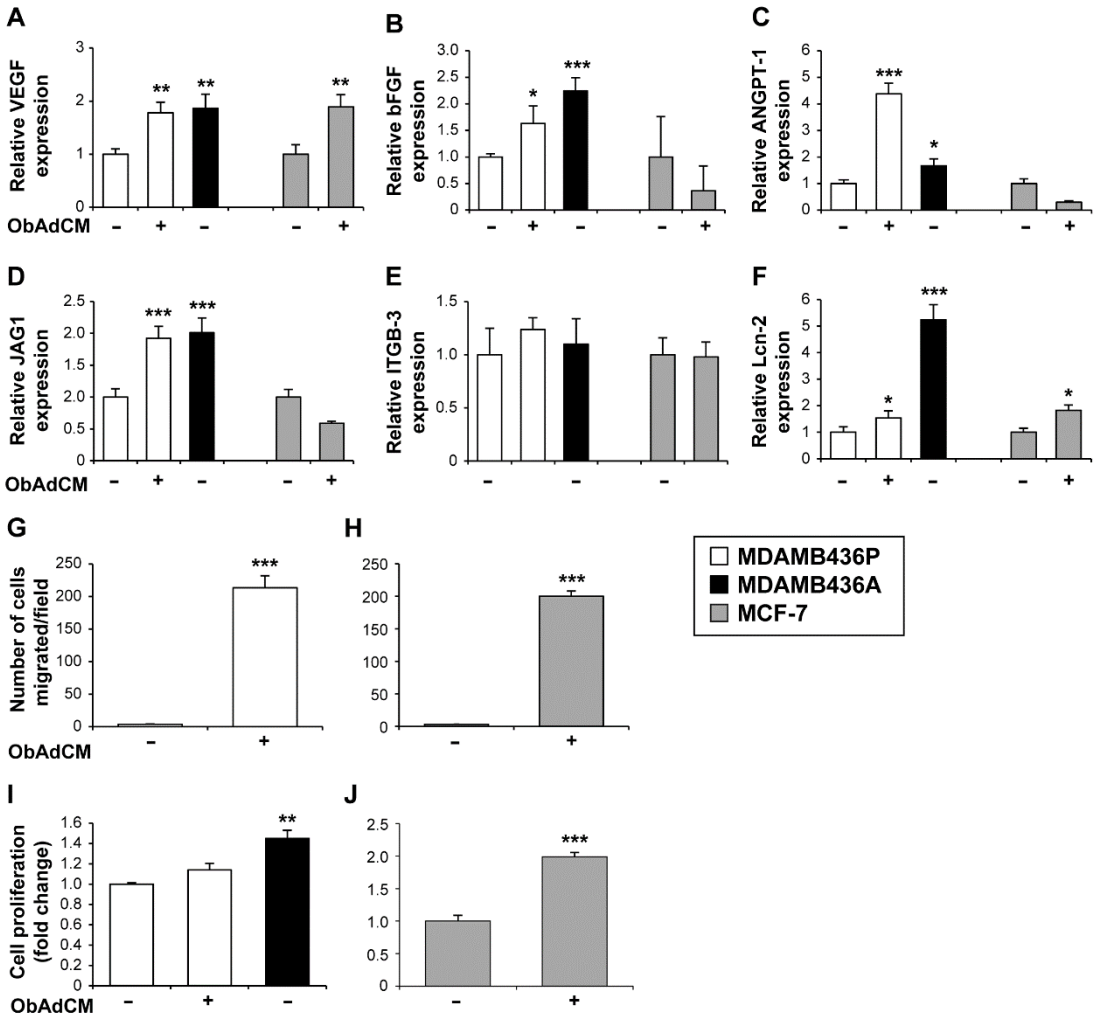

Figure S6. **ObAdCM treatment induced the expression of pro-angiogenic factors in BC cells**. Treatment with ObAdCM increased mRNA expression of pro-angiogenic factors such as VEGF (**A**), bFGF (**B**), ANGPT-1 (**C**), JAG1 (**D**) and LCN2 (**F**) in dormant MDA-MB-436P as well as non-aggressive MCF-7 cells. mRNA levels of integrin beta3 did not differ (**E**). ObAdCM treatment significantly increased migration of MDA-MB-436P (**G**) and MCF-7 (**H**) BC cells. ObAdCM treatment did not increase MDA-MB-436P cell proliferation (**I**), however, proliferation of MCF-7 was increased (**J**). All experiments were conducted at least three times. Students t test, significance $P^{*} \leq 0.05$, $^{**} \leq 0.01$, $^{*} \leq 0.001$.

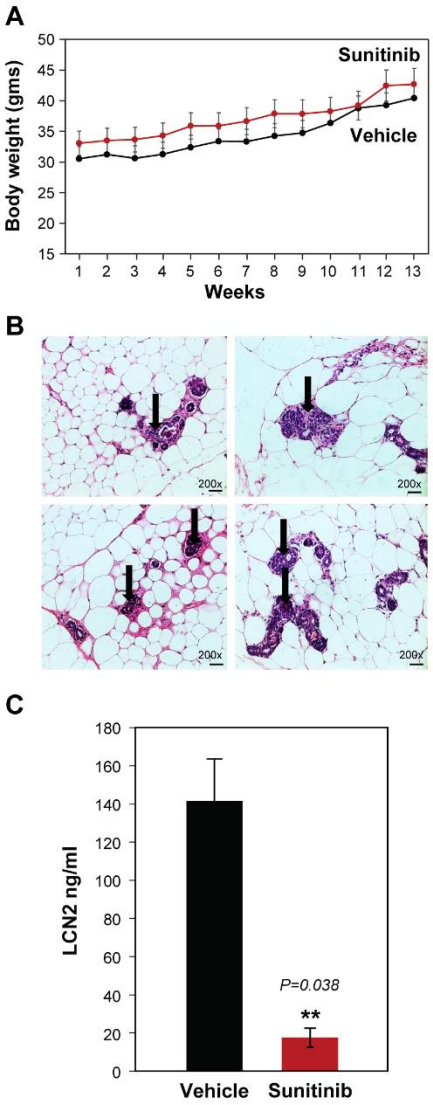

Figure S7. **Sunitinib treatment delays or inhibits tumor initiation in DIO MTB-TWNT BC model**. Sunitinib treatment did not affect weight gain (**A**, black dot, vehicle, red dot, sunitinib). MFP in sunitinib-treated mice had multiple lesions arrested at the hyperplastic or *in situ* stages (**B**, arrows). Serum levels of LCN2 were significantly lower in sunitinib-treated mice (**C**, n=4/group, Students t test, *P*=0.038).

Supplementary Tables

Table S1. MTB-TWNT endpoint tumor biomarker levels.

Angiogenic markers	NC	DIO	*P*	Fold-change (DIO/NC)
VEGF pg/ml	555 (358.5 – 843.5)	2393 (2330.2 – 2403.1)	0.003*	4.3
bFGF ng/ml	4.9 (4.5 – 15.5)	11.8 (9.5 – 13.1)	0.94	2.4
IL-6 pg/ml	ND[I]	ND	--	--
LCN2 ng/ml	16836 (8637 – 17097)	14869 (8338 - 25702)	0.62	0.8
Tsp-1 ng/ml	572.1 (561.5 – 803.6)	611.7 (535.2 – 838.1)	0.97	1.0

Data are median (IQR) with comparisons based on Wilcoxon signed-ranks test for matched samples.
*Statistically significant increase. [I]Not detectable.

Table S2. MTB-TWNT endpoint serum biomarker levels.

Angiogenic markers	NC	DIO	*P*	Fold-change (DIO/NC)
VEGF pg/ml	33.0 (25.3 – 39.2)	53 (40.1 - 61.3)	0.11	1.60
bFGF pg/ml	489.5 (349 – 656.8)	736.3 (676 – 916.1)	0.15	1.40
IL-6 pg/ml	39.1 (25.1 – 51.6)	46.5 (25.7 – 49.2)	0.53	1.20
LCN2 ng/ml	130.6 (116.6 -168.7)	3209 (3014.3 – 3111.7)	0.005*	14.82
Tsp-1 ng/ml	165.5 (89 – 243.2)	96.4 (81 – 144.5)	0.18	0.58

Data are median (IQR) with comparisons based on Wilcoxon signed-ranks test for matched samples.
*Statistically significant increase.

Table S3. MDA-MB-436P endpoint tumor biomarker levels.

Angiogenic markers	NC	DIO	Fold-change (DIO/NC)	*P*
VEGF pg/mL	164.6 (119.6 – 271.7)	68.9 (46.4 – 203.3)	0.41	0.59
bFGF pg/ml				
IL-6, ng/mL	7360 (4665 – 10037)	7929 (5111 – 11963)	1.07	0.79
Tsp-1, ng/ml	155.3 (108.4 – 865.9)	61.1 (30.5 – 107.4)	0.40	0.41
LCN2, ng/ml	ND[I]	5.96 (5.5-7.6)	-	0.005*

Data are median (IQR) with comparisons based on Wilcoxon signed-ranks test for matched samples. *Statistically significant increase. [I]ND not detectable.

Table S4. MDA-MB-436P endpoint serum biomarker levels.

Angiogenic markers	NC	DIO	*P*	Fold-change (DIO/NC)
VEGF pg/ml	15.6 (6.4 – 23)	15.9 (12 – 23)	0.78	1.01
bFGF pg/ml	713.3 (697.2 – 732.3)	868.8 (759.2 – 2536.3)	0.88	1.21
IL-6 pg/ml	7.5 (5 – 16.4)	24.8 (22.1 – 27.7)	0.30	3.30
LCN2 ng/ml	4729.7 (3273 – 11312.8)	13909.2 (5874 – 15806)	0.25	2.94
Tsp-1 ng/ml	90.6 (77 – 115.1)	143.7 (118.1 – 167.4)	0.43	1.58

Data are median (IQR) with comparisons based on Wilcoxon signed-ranks test for matched samples. *Statistically significant increase.

Supplementary References

1. N. P. Nunez, S. N. Perkins, N. C. Smith, D. Berrigan, D. M. Berendes, L. Varticovski, J. C. Barrett, S. D. Hursting, Obesity accelerates mouse mammary tumor growth in the absence of ovarian hormones. *Nutrition and cancer* **60**, 534-541 (2008).
2. R. Roy, S. Rodig, D. Bielenberg, D. Zurakowski, M. A. Moses, ADAM12 transmembrane and secreted isoforms promote breast tumor growth: a distinct role for ADAM12-S protein in tumor metastasis. *Journal of Biological Chemistry* **286**, 20758-20768 (2011).
3. J. Yang, D. R. Bielenberg, S. J. Rodig, R. Doiron, M. C. Clifton, A. L. Kung, R. K. Strong, D. Zurakowski, M. A. Moses, Lipocalin 2 promotes breast cancer progression. *Proceedings of the National Academy of Sciences* **106**, 3913-3918 (2009).
4. E. J. Gunther, G. K. Belka, G. B. Wertheim, J. Wang, J. L. Hartman, R. B. Boxer, L. A. Chodosh, A novel doxycycline-inducible system for the transgenic analysis of mammary gland biology. *The FASEB Journal* **16**, 283-292 (2002).
5. E. J. Gunther, S. E. Moody, G. K. Belka, K. T. Hahn, N. Innocent, K. D. Dugan, R. D. Cardiff, L. A. Chodosh, Impact of p53 loss on reversal and recurrence of conditional Wnt-induced tumorigenesis. *Genes & development* **17**, 488-501 (2003).
6. B. K. Jha, B. Dong, C. T. Nguyen, I. Polyakova, R. H. Silverman, Suppression of antiviral innate immunity by sunitinib enhances oncolytic virotherapy. *Molecular Therapy* **21**, 1749-1757 (2013).
7. J. W. Wragg, V. L. Heath, R. Bicknell, Sunitinib treatment enhances metastasis of innately drug-resistant breast tumors. *Cancer research* **77**, 1008-1020 (2017).
8. G. N. Naumov, L. A. Akslen, J. Folkman, Role of angiogenesis in human tumor dormancy: animal models of the angiogenic switch. *Cell cycle* **5**, 1779-1787 (2006).

9. G. N. Naumov, E. Bender, D. Zurakowski, S.-Y. Kang, D. Sampson, E. Flynn, R. S. Watnick, O. Straume, L. A. Akslen, J. Folkman, A model of human tumor dormancy: an angiogenic switch from the nonangiogenic phenotype. *Journal of the National Cancer Institute* **98**, 316-325 (2006).

10. J. Harper, G. N. Naumov, A. Exarhopoulos, E. Bender, G. Louis, J. Folkman, M. A. Moses. (AACR, 2006).

11. R. Roy, A. Dagher, C. Butterfield, M. A. Moses, ADAM12 is a novel regulator of tumor angiogenesis via STAT3 signaling. *Molecular Cancer Research* **15**, 1608-1622 (2017).

12. M. A. Moses, D. Wiederschain, K. R. Loughlin, D. Zurakowski, C. C. Lamb, M. R. Freeman, Increased incidence of matrix metalloproteinases in urine of cancer patients. *Cancer research* **58**, 1395-1399 (1998).

13. R. Roy, M. A. Moses, ADAM12 induces estrogen-independence in breast cancer cells. *Breast cancer research and treatment* **131**, 731-741 (2012).